Solid-liquid phase transition in argon

Tung Tsang and Hwa T. Tang
Department of Physics and Astronomy, Howard University, Washington, D. C. 20059
and Department of Mathematics, California State University, Hayward, California 94542
(Received 26 May 1978)

Starting from the Lennard-Jones interatomic potential, a modified cell theory has been used to describe the solid-liquid phase transition in argon. The cell-size variations may be evaluated by a self-consistent condition. With the inclusion of cell-size variations, the transition temperature, the solid and liquid densities, and the liquid-phase radial-distribution functions have been calculated. These *ab initio* results are in satisfactory agreement with molecular-dynamics calculations as well as experimental data on argon.

I. INTRODUCTION

The melting of solids and the freezing of liquids are very common phenomena of fundamental importance. It is somewhat surprising that the solid-liquid phase transition is still poorly understood at present from the point of view of first principles. The literature is also somewhat sparse, and it is often necessary to rely on molecular dynamics or Monte Carlo computer experiments for quantitative results.[1-6]

Recently, Barker and Henderson[7] have pointed out that apart from the Monte Carlo calculations, most current theories of melting have either used different models for solid and fluid phases or used the known melting properties of hard spheres to predict those of more realistic systems. Barker and Henderson have also emphasized that our theoretical understanding of the melting transition would require a unified description of the solid and the fluid as well as the phase transition. Whereas the physics of the liquid state has been very extensively studied and has been comprehensively reviewed,[1,7-9] the derivation of such a unified description may not be easy. Among the current theories of the liquid state, a perturbation theory approach to the melting transition would rely heavily on the computer simulation results for phase transitions in hard-sphere systems, whereas the integral equation approaches have had difficulties with the various approximations involved in these calculations.

In our present work, the melting transition of a simple Lennard-Jones system has been studied by a modified cell theory. The cell theory, originated by Lennard-Jones and Devonshire, has been reviewed in great detail by Barker and Hirschfelder *et al.*[7,10,11] It is well known that the solid states of the rare gases have the face-centered cubic (fcc) structure. In the cell model for the liquid state, each particle was located in the potential well of its own Wigner-Seitz (WS) cell of the fcc structure. The WS cell is a regular dodecahedron.[12] The cell model is currently out of favor because it is unrealistic to have highly regular dodoechedrons of identical sizes in any fluid which is known to possess certain degrees of randomness. On the other hand, the cell model does use quite similar descriptions for both the liquid and the solid state. In recent years, Barker and others[13-16] have developed self-consistent cell theories and these theories have been applied to hard-sphere systems with good results. In our present work, a more simplified self-consistent condition has been used. We have allowed for random variations in distorted dodoecahedron cells of various sizes and a self-consistent condition is imposed on these variations. Because of its simplicity, it is possible to study the melting transitions in systems with realistic interatomic potentials such as Lennard-Jones systems or argon. In Sec. II, the general formulation of the problem and the self-consistent condition have been given. In Sec. III, the single-particle potentials and partition functions have been evaluated. We have calculated the potentials in the WS cell and have then taken the angular average by lattice-harmonics procedures, thus avoiding the smearing approximation[10,11] about the replacement of the dodecahedron by a sphere of uncertain size. The melting transition was derived from the modified cell model in Sec. IV and was then compared with the experimental data. In Sec. V, the radial distribution function $g(R)$ was evaluated for the liquid phase and was then compared with the molecular-dynamics calculations and experimental data. The main features are then discussed in Sec. VI.

The Lennard-Jones interatomic potential $v(R)$ is given by

$$v(R) = 4\epsilon[(\sigma/R)^{12} - (\sigma/R)^{6}],$$

where R is the interatomic distance, σ and ϵ are the Lennard-Jones diameter and well depth, respectively. For argon, the standard choice[11,17] is $\sigma = 3.4\times10^{-8}$ cm and $\epsilon/k = 120$°K, where k is the Boltzmann constant. Following the standard conventions of Hirschfelder and others,[11] we will use the mass of an argon atom $m = 6.63\times10^{-23}$ g as the mass unit, $\sigma = 3.4\times10^{-8}$ cm as the distance unit, $\epsilon = 1.657\times10^{-14}$ erg as the energy unit, and 1.680 g/cm^3 as the density unit. In these units, the interactomic potential is

$$v(R) = 4(R^{-12} - R^{-6}) . \tag{1}$$

We will also use the reduced temperature $T^* = kT/\epsilon$ in place of the temperature T in °K. In our units, we may replace kT by T^*.

II. GENERAL FORMULATION

For a system of N classical particles, the potential energy of the system in $U(\vec{R}_1\cdots\vec{R}_N) = \sum v_{ij}$, where $v_{ij} = v(R_{ij})$, $\vec{R}_{ij} = \vec{R}_j - \vec{R}_i$, and the summation is over $i<j=1$ to N. The classical partition function Z_N is

$$Z_N = (h^2/2\pi mkT)^{-3N/2} Q_N , \tag{2}$$

where Q_N is the configurational integral or configurational partition function

$$Q_N = \int\cdots\int e^{-U/T^*} d\vec{R}_1\cdots d\vec{R}_N . \tag{3}$$

The Helmholtz free energy is given by

$$A = -kT\ln Z_N = -\tfrac{3}{2}N\ln(h^2/2\pi mkT) + Nf , \tag{4}$$

where f may be regarded as the configurational free energy per particle

$$f = -(kT\ln Q_N)/N . \tag{5}$$

In order to evaluate the many-body integral Q_N, it is convenient to approximate the many-body potential U as a sum of single-body potentials

$$U(\vec{R}_1\cdots\vec{R}_N) = \sum_i V_i(\vec{R}_i) . \tag{6}$$

The simplest choice for the single-particle potential V_i is[10,16]

$$V_i = \frac{1}{2}\sum_j v_{ij} . \tag{7}$$

The single-particle potential will now be evaluated. We will focus our attention on the most important contributions from the nearest neighbors (NN) of particle i. (Contributions from other neighbors will be discussed in the next section.) In the original Lennard-Jones and Devonshire cell theory, the fcc structure was used with identical nearest-neighbor distances a. The WS cell with NN distance a is a regular dodecahedron of volume $a^3/\sqrt{2}$. If the most probable position of particle i was defined as the origin, then the neighbors $j_1\cdots j_{12}$ were fixed at $(\pm a/\sqrt{2}, \pm a/\sqrt{2}, 0)$, $(\pm a/\sqrt{2}, 0, \pm a/\sqrt{2})$, and $(0, \pm a/\sqrt{2}, \pm a/\sqrt{2})$. The configuration partition function is then evaluated by allowing particle i to move away from origin. However, since liquid structures are not perfectly regular, it is necessary to consider the WS cells as distorted dodecahedrons of various sizes. We will consider the system of N particles at some particular instant. Let us denote the nearest neighbors of particle i as $j = 1, 2, \ldots, 12$. Then the NN distances are

$$a_{ij} = R_{ij} = |\vec{R}_j - \vec{R}_i| , \quad j = 1, \ldots, 12 . \tag{8}$$

The cell for particle i may be defined as the polyhedron enclosed by the bisecting planes. We may approximate this cell by a WS cell of regular octahedron with volume $\alpha_i^3/\sqrt{2}$ where α_i is the average (over $j = 1$–12) value of a_{ij},

$$\alpha_i = \langle a_{ij}\rangle_j = \langle R_{ij}\rangle_j = \langle|\vec{R}_j - \vec{R}_i|\rangle_j . \tag{9}$$

The center of the WS cell may be defined as the center of mass $\langle\vec{R}_j\rangle_j$ of the 12 nearest neighbors. The position of particle i relative to the WS cell center is then

$$\vec{r}_i = \vec{R}_i - \langle\vec{R}_j\rangle_j . \tag{10}$$

For the system with N particles, the number of WS cells with volume between $\alpha^3/\sqrt{2}$ and $(\alpha+d\alpha)^3/\sqrt{2}$ will be defined as $Np(\alpha)\,d\alpha$, where $p(\alpha)$ is the normalized probability. The density ρ of the system is well approximated by using the average cell parameter $\alpha_A = \int \alpha p(\alpha)\,d\alpha$,

$$\rho = \sqrt{2}/\alpha_A^3 . \tag{11}$$

The probability function $p(\alpha)$ may be approximated by a Gaussian function with root-mean-square (rms) deviation α':

$$p(\alpha) = (2\pi\alpha'^2)^{-1/2}\exp[-(\alpha-\alpha_A)^2/2\alpha'^2] , \tag{12}$$

where $\alpha'^2 = \int(\alpha-\alpha_A)^2 p(\alpha)\,d\alpha$, the integration limits being $\alpha = 0$ to ∞.

From (9) and (10), a self-consistent condition may be established for α' by examining the population distributions and rms deviations of $\vec{R}_i$, $\vec{r}_i$, and α_i. From (10), the rms deviations of $\vec{r}_i$ and $\vec{R}_i$ are expected to be very similar since $\langle\vec{R}_j\rangle_j$ is an average of 12 positions with much smaller rms deviations. From (9), the distance R_{ij} is from the difference between two radius vectors, whereas α_i is the average of twelve R_{ij} distances. Conventional probability theory gives

$$\alpha'^2 = \tfrac{2}{12}\langle r^2\rangle = \tfrac{1}{6}\langle r^2\rangle , \tag{13}$$

where $\langle r^2\rangle$ is the canonical average value of r^2.

We may define $\langle r^2\rangle_\alpha$ as the canonical average value of r^2 for WS cell of fixed volume $\alpha^3/\sqrt{2}$, then we have the self-consistent condition

$$6\alpha'^2 = \langle r^2\rangle = \int \langle r^2\rangle_\alpha p(\alpha)\, d\alpha\,. \tag{14}$$

In Sec. III we will evaluate $\langle r^2\rangle_\alpha$ as a function of α and T^*. For any given α_A, then the rms deviation α' and the probability function $p(\alpha)$ may be calculated from (12) and (14). As a result of (6), the configurational partition function Q_N may be written as a product of single-cell configurational partition functions Q_1:

$$\ln Q_N = N\int p(\alpha)\ln Q_1(\alpha)\, d\alpha\,, \tag{15}$$

where Q_1 is a function of the cell parameter α. This is a modification of the original cell theory where only one cell size is considered:

$$\ln Q_N = N\ln Q_1(\alpha_A)\,. \tag{16}$$

III. SINGLE-PARTICLE FUNCTIONS

We may write $V_i = V_i' + V_i''$, where V_i' and V_i'' are the NN contributions and the contributions from other particles, respectively. The potential V_i'' is only slightly dependent on the detailed structure of the N particle system, thus the structure may be approximated by the regular fcc lattice with NN distance α. Thus we get

$$2V'' = 6v(\sqrt{2}\alpha) + 24v(\sqrt{3}\alpha) + 12v(2\alpha) + 24v(\sqrt{5}\alpha) + 8v(\sqrt{6}\alpha) + 48v(\sqrt{7}\alpha) + 6v(\sqrt{8}\alpha) + \cdots, \tag{17}$$

with the particles farther away than $\sqrt{8}\alpha$ replaced by a uniform fluid of density $\sqrt{2}\alpha^{-3}$.

We will now evaluate $V'(x, y, z)$ inside a WS cell of regular octahedron with volume of $\alpha^3/\sqrt{2}$ and

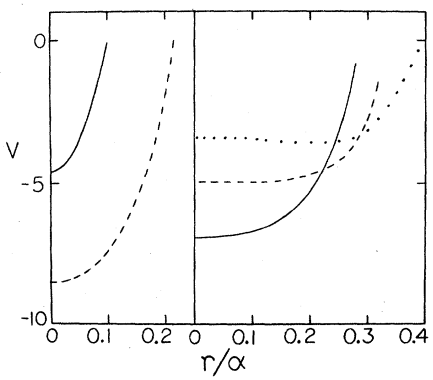

FIG. 1. Cell potential V vs r/α. Left: solid line, $\alpha=1$; dashed line, $\alpha=1.1$. Right: solid line, $\alpha=1.2$; dashed line, $\alpha=1.3$; dotted line, $\alpha=1.4$.

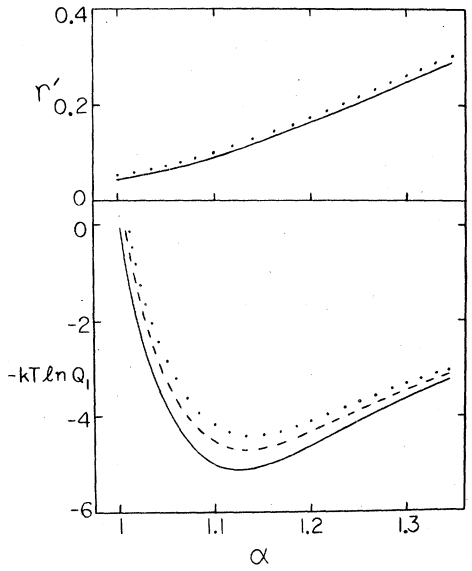

FIG. 2. $r' = (\langle r^2\rangle)^{1/2}$ (top figure) and $-kT\ln Q_1$ (bottom figure) vs cell parameter for fixed cell size. Solid lines, $T^*=0.6$; dashed lines, $T^*=0.7$; dotted lines, $T^*=0.786$.

with center at the origin. It is convenient to retain only the isotropic part of $V'(x, y, z)$; that is, we average $V'(x, y, z)$ to obtain $V'(r)$. The WS cell has cubic symmetry, hence the lattice harmonics[18,19] may be used for the spherical-harmonics expansion of $V'(x, y, z)$:

$$V'(x,y,z) = V_0 + V_4(\bar{x}^4+\bar{y}^4+\bar{z}^4-\tfrac{3}{5}) + V_6[\bar{x}^2\bar{y}^2\bar{z}^2 + \tfrac{1}{22}(\bar{x}^4+\bar{y}^4+\bar{z}^4-\tfrac{3}{5}) - \tfrac{1}{105}] + \cdots, \tag{18}$$

where $V_0, V_4, V_6, \ldots$ are function of r only and $\bar{x}=x/r$, $\bar{y}=y/r$, and $\bar{z}=z/r$ are the direction cosines. We have evaluated V' along the [100], [110], and [111] axis, and then we use

$$V'(r) = 0.286V'(x=r, y=0, z=0) + 0.457V'(x=r/\sqrt{2}, y=r/\sqrt{2}, z=0) + 0.257V'(x=r/\sqrt{3}, y=r/\sqrt{3}, z=r/\sqrt{3})\,, \tag{19}$$

where the coefficients are chosen such that the V_4 and V_6 terms average to zero. The cell potential V is the sum of V' and V'' given by (19) and (17).

The cell potential $V(r)$ is shown in Fig. 1 for the regular dodecahedral WS cell at several different values of cell parameter α. Our results are in general agreement with previous calculations.[11] From our cell potential $V(r)$, it is then

possible to calculate the single-cell partition function $Q_1(\alpha)$ at any fixed temperature T^*:

$$Q_1(\alpha) = \int 4\pi r^2 e^{-V(r)/T^*}\, dr\,, \tag{20}$$

where the $V(r)$ is for a WS cell with cell parameter α. For cell models with fixed cell sizes, we have

$$f(\alpha) = -kT \ln Q_1(\alpha)\,. \tag{21}$$

In addition, we have

$$\langle r^2\rangle_\alpha = \left(\int r^4 e^{-V(r)/T^*}\, dr\right)\Big/\left(\int r^2 e^{-V(r)/T^*}\, dr\right). \tag{22}$$

In Fig. 2, we have shown $r' = (\langle r^2\rangle)^{1/2}$ and $-kT \ln Q_1$ (the configurational free energy per particle for fixed cell size) as a function of cell parameter α for $T^* = 0.6$, 0.7, and 0.786. The curves are quite similar to each other and there is no phase transition.

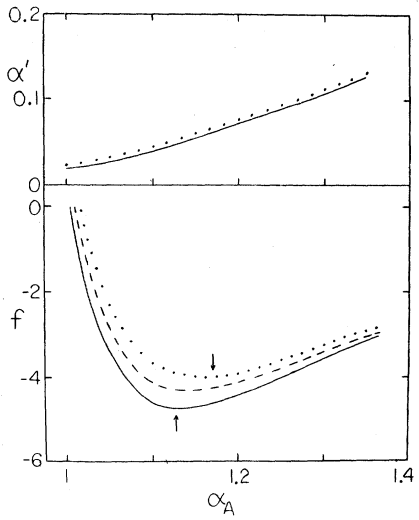

FIG. 3. Cell-parameter variation α' (top figure) and configurational free energy f (bottom figure) vs average cell parameter α_A. Solid lines, $T^* = 0.6$; dashed lines, $T^* = 0.7$; dotted lines, $T^* = 0.786$.

IV. MELTING TRANSITION

Taking into account the variations in cell sizes, we may evaluate the configurational free energy per particle $f = (-kT \ln Q_N)/N$ from (12) and (15) using the results for Q_1 from Sec. III (Fig. 2). The rms deviation α' in cell parameter may be determined from the self-consistent condition (15). Our results for f as a function of average cell parameter α_A are shown in the lower diagram of Fig. 3 for several temperatures. The most stable configuration corresponds to the free-energy minimum. For $T^* = 0.7$ (dashed curve), we note that the minimum is rather flat between $\alpha_A = 1.12$ and $\alpha_A = 1.17$. As a result of the flatness of this minimum region, there is an abrupt shift of the minimum toward small α_A at slightly lower temperatures (solid curve) and also an abrupt shift toward large α_A at slightly higher temperatures (dotted curve). This rather abrupt, although still continuous, change in average cell size occurred near $T^* = 0.7$ and may be identified with the melting transition. The low-temperature phase, with average cell parameter $\alpha_A = 1.13$ and density $\rho = \sqrt{2}\alpha_A^{-3} = 0.98$ (at the minimum of the solid curve indicated by an arrow), may be identified with solid argon. The high-temperature phase, with $\alpha_A = 1.17$ and $\rho = \sqrt{2}\alpha_A^{-3} = 0.88$ (at the minimum of the dotted curve indicated by an arrow), may be identified with the liquid phase. There is an abrupt volume expansion (~10%) accompanying the melting transition.

Our calculated melting temperature $T^* = 0.7$, and the solid and liquid densities, $\rho = 0.98$ and 0.88, are consistent with experimental values[1] for argon at low pressure, $T^* = 0.70$, $\rho = 0.96$ and 0.84, and are also consistent with molecular-dynamics values for Lennard-Jones systems, $T^* = 0.67$, $\rho = 0.96$ and 0.86.

We note that the phase transition does not occur if the self-consistent condition is omitted and all cells are assumed to be of uniform size. From the lower diagram of Fig. 2, the minimum of $-kT \ln Q_1$ vs α is much sharper and the change of the position of minimum is rather gradual. Thus the Lennard-Jones and Devonshire cell model is usually identified with the disordered solid.[10]

V. RADIAL DISTRIBUTION FUNCTION OF LIQUID ARGON

Let us consider the NN radial distribution function $g_1(R, \alpha)$ for a system with fixed cell size of volume $\alpha^3/\sqrt{2}$, where R is the NN distance. If the 12 nearest neighbors were replaced by a uniform spherical distribution at a constant distance α from the center, then the rms deviation β in NN distances will be $r/\sqrt{3}$ for $r \ll \alpha$ if the center particle is displaced by distance r from the cell center. The result for regular dodecahedral coordination of nearest neighbors is also very similar. In the Gaussian approximation, the distribution function g_1 is then given by

$$4\pi R^2 g_1(R, \alpha) = 12 e^{-(R-\alpha)^2/2\beta^2}/(2\pi)^{1/2}\beta\,, \tag{23}$$

Where $\beta^2 = \frac{1}{3}r'^2 = \frac{1}{3}\langle r^2\rangle$ and r' is shown as a function of α in top diagram of Fig. 2. It is also necessary

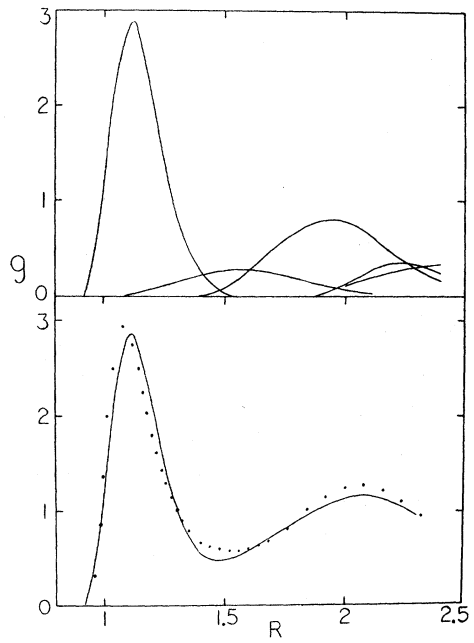

FIG. 4. Radial distribution $g(R)$ vs R in the liquid state, $T^*=0.786$. Top, from left to right: g_1, g_2, $\cdots$, g_5 for the first five neighboring shells. Bottom: solid line, $g(R)=g_1+g_2+\cdots+g_5$; dotted line, molecular-dynamics results of Verlet, Ref. 20.

to take into account the variation in cell sizes, thus we get

$$g_1(R)=\int p(\alpha)g_1(R,\alpha)\,d\alpha\,, \tag{24}$$

with $p(\alpha)$ given by (12). For the liquid state, we have $\alpha_A=1.17$, and the distribution function $g_1(R)$ from (24) is shown at the top left of Fig. 4.

In the fcc lattice, there are six second-nearest neighbors at distance $\sqrt{2}\alpha$ (two NN distances at bond angle of 90°). If the bond angle is fixed at 90°, then the second NN distribution function $g_2(R)$ is given by

$$\tfrac{1}{6}g_2(R)=\tfrac{1}{12}g_1(R/\sqrt{2})/(\sqrt{2})^3\,. \tag{25}$$

It is also necessary to take into account the bond angle variations. If we have three nearest neighbors forming an equilateral triangle, then the bond angle is 60° with rms deviation of 10° from the NN distribution function $g_1(R)$. Using the bond angle 90° with rms of 15° for second-nearest neighbors, the distribution function $g_2(R)$ has been calculated and has been shown in the top diagram of Fig. 4.

In the fcc lattice, the third, fourth, and fifth neighbors are located at $\sqrt{3}\alpha$, 2α, and $\sqrt{5}\alpha$, and there are 24, 12, and 24 particles, respectively. The distribution functions g_3, g_4, and g_5 have been calculated and have also been shown in Fig. 4.

In the bottom diagram of Fig. 4, the solid line is the calculated radial distribution function $g(R)=g_1(R)+\cdots+g_5(R)$. Our calculated $g(R)$ may be compared with the molecular-dynamics calculations of Verlet[20] which is shown as the dotted line. (Verlet's result is quite similar to other molecular-dynamics calculations[17] and is also quite similar to x-ray and neturon-diffraction experimental data[21,22] on liquid argon.) There is reasonably good agreement.

VI. DISCUSSION

The original Lennard-Jones and Devonshire cell model has assumed WS cells of identical shape (regular dodecahedron) and size. In order to describe the liquid-solid phase transitions, however, it is necessary to introduce disordered structures. In our present work, we have used a self-consistent condition for the distribution of cell sizes. From this cell-size distribution, it is then possible to describe the solid-liquid transition in a very simple way. From Fig. 1, the structures with smaller cells ($\alpha\sim1.1$) have lower energies, whereas the structures with larger cells ($\alpha\sim1.2$) have larger free volumes. Hence the former structure is more favorable at lower temperatures while the latter is preferred at higher temperatures. Near the transition temperature, the free energy versus cell parameter curve has a rather flat minimum (Fig. 3) and therefore this transition is rather abrupt. Our results are in satisfactory agreement with molecular-dynamics calculations as well as experimental data on argon. The transition in our model is abrupt although still continuous and is not quite as sharp as a first-order phase transition.

We have also shown that the modified cell model can describe the radial distribution function $g(R)$ of the liquid state reasonably well. In addition, it is possible to explain why the most prominent peaks of $g(R)$ near $R\sim1.1$ for liquids and solids are quite similar despite the approximately 10% volume expansion on melting. As compared to the solid phase, there is more variation of cell sizes in the liquid phase. Since small cells tend to contribute sharper peaks to $g(R)$, the radial distribution function peak from nearest neighbors are shifted toward smaller distances.

It is somewhat arbitrary to describe the liquid state by a distorted fcc lattice. Therefore, there is deviation between our radial distribution function $g(R)$ and the molecular dynamics data. In particular, the deviation near $R=1.5$ suggests that the fcc lattice approximation underestimates the

particle density in the second coordination shell.

In summary, a modified cell theory can describe the melting transition as well as the liquid structure in reasonable agreement with molecular-dynamics calculations and experimental data on argon.

ACKNOWLEDGMENT

This work was partially supported by National Aeronautics and Space Administration under Grants No. NGR-09-011-057 and NSG 5186. These financial supports are gratefully acknowledged.

[1]J. P. Hansen and I. R. McDonald, *Theory of Simple Liquids* (Academic, New York, 1976).
[2]A. R. J. P. Ubbelohde, Adv. Chem. Phys. 6, 459 (1964).
[3]B. Jancovici, in *Fundamental Problems in Statistical Mechanics*, edited by E. G. D. Cohen (Interscience, New York, 1968), p. 106.
[4]W. B. Streett, H. J. Raveche, and R. D. Mountain, J. Chem. Phys. 61, 1960 (1974).
[5]H. J. Raveche, R. D. Mountain, and W. B. Streett, J. Chem. Phys. 61, 1970 (1974).
[6]D. E. O'Reilly, Phys. Rev. A 15, 1198 (1977).
[7]J. A. Barker and D. Henderson, Rev. Mod. Phys. 48, 587 (1976).
[8]C. A. Croxton, *Liquid State Physics* (Cambridge U.P., London, 1974).
[9]R. O. Watts and I. J. McGee, *Liquid State Chemical Physics* (Wiley, New York, 1976).
[10]J. A. Barker, *Lattice Theories of the Liquid State* (Pergamon, Oxford, 1963).
[11]J. O. Hirschfelder, C. F. Curtiss, and R. B. Bird, *Molecular Theory of Gases and Liquids* (Wiley, New York, 1954).
[12]Reference 11, p. 287, Fig. 4.6-1.
[13]J. A. Barker, J. Chem. Phys. 44, 4212 (1966).
[14]J. A. Barker, J. Chem. Phys. 63, 632 (1975).
[15]J. A. Barker and H. M. Gladney, J. Chem. Phys. 63, 3870 (1975).
[16]M. Fixman, J. Chem. Phys. 51, 3270 (1969).
[17]A. Rahman, Phys. Rev. 136, A405 (1964).
[18]D. G. Bell, Rev. Mod. Phys. 26, 311 (1954).
[19]F. C. Von der Lage and H. Bethe, Phys. Rev. 71, 612 (1947).
[20]L. Verlet, Phys. Rev. 165, 201 (1968).
[21]J. F. Karnicky and C. J. Pings, Adv. Chem. Phys. 34, 157 (1976).
[22]J. L. Yarnell, M. J. Katz, R. G. Wenzel, and S. H. Koenig, Phys. Rev. A 7, 2130 (1973).